

Supplementary Materials for

Predicting Fracture Energies and Crack-Tip Fields of Soft Tough Materials

Teng Zhang^{1,a)}, Shaoting Lin^{1,a)}, Hyunwoo Yuk¹, Xuanhe Zhao^{1,2, b)}

¹ Soft Active Materials Laboratory, Department of Mechanical Engineering, Massachusetts Institute of Technology, Cambridge, MA 02139, USA; ² Department of Civil and Environmental Engineering, Massachusetts Institute of Technology, Cambridge, MA 02139, USA

a) These authors contribute equally to this work

b) To whom correspondence should be addressed. Email: zhaox@mit.edu

Pure-shear test for the measurement of fracture energy

To measure the fracture energy of the samples, we separately stretch two identical samples with the same thickness T_0 , width W_0 and initial gage length L_0 , where $W_0 \gg L_0 \gg T_0$ (see **Fig. S1**). One sample is notched with a crack length ranging from $0.25W_0$ to $0.5W_0$ and the other is un-notched. The notched sample is stretched to a critical distance L_c until crack starts to propagate while the un-notched sample is stretched to measure the force-displacement curve.

The fracture energy of the gel can be calculated by $\Gamma = \int_{L_0}^{L_c} F dl / (W_0 T_0)$ [1].

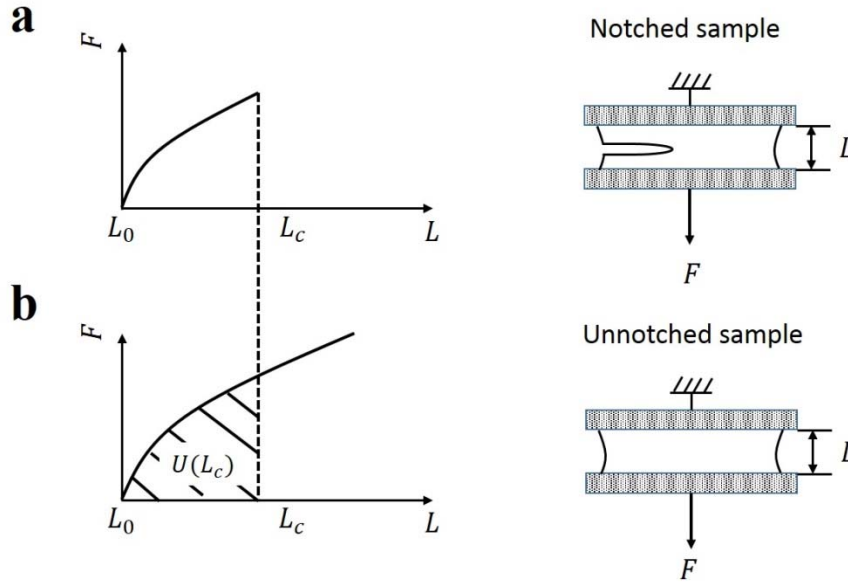


Figure S1. Schematic of pure-shear test for measuring fracture energy of hydrogels. (a)

Notched samples are stretched to critical distance of L_c until the crack propagates. (b) Un-

notched samples are stretched to L_c with the force F recorded and the fracture energy of the

hydrogel can be calculated as $\Gamma = (\int_{L_0}^{L_c} F dl) / (W_0 T_0)$, where W_0 , T_0 and L_0 represents width,

thickness and initial gage length of the sample, respectively.

Finite-element models

We implemented the coupled cohesive-zone and Mullins-effect model into a two-dimensional (2D) finite-element model to simulate the pure-shear test of soft materials. As shown in **Fig. S2**, the numerical model consists of a finite strip with a height of L_0 , width of W_0

and an initial crack length of a . The geometry of the simulated strip is taken as $L_0=60$ mm, $W_0=480$ mm, and $a =120$ mm unless otherwise specified. The pure elastic properties the hydrogel were modeled as the one term Ogden hyperelastic material [2]

$$\tilde{W} = 2\mu/\alpha_1^2 \left(\lambda_1^{\alpha_1} + \lambda_2^{\alpha_1} + \lambda_3^{\alpha_1} - 3 \right) \quad (\text{S1})$$

where μ is the shear modulus, α_1 a fitting parameter and λ_i the i_{th} principle stretch ($i=1,2,3$). A Neo-Hookean material model (i.e., $\alpha_1 = 2$) is first adopted as the model material to gain theoretical understanding of the toughness enhancement due to energy dissipation. Also, it has been shown that Eq. (S1) can accurately capture the elastic deformation of the hydrogels used in current study (**Fig. 5a** and **Fig. S5**).

All the finite-element calculations are performed with ABAQUS/Explicit. Since the explicit simulations cannot handle fully incompressible materials, we set the Poisson's ratio of the soft materials to be larger than 0.499. The soft material is modeled using plane-stress 4-node linear elements with reduced integration (CPS4R). The cohesive interaction for describing crack propagation is described with the cohesive element implemented in ABAQUS (COH2D). The crack surface is uniformly discretized with very fine mesh (0.1 mm). The hydrogel strip is loaded by fixing the displacement along horizontal direction of the top and bottom surfaces and moving them along vertical direction with a constant velocity. A very low loading rate is adopted to ensure a quasistatic process, which can be verified by the stress-stretch curves from simulations under different loading rates (**Fig. S2a**). The maximum stress point on the stress-stretch curve is used to calculate the fracture energy according to the pure-shear method described above. As shown in **Fig. S2b-c**, the failures of the materials with and without the Mullins effect occur at critical stretch ratios around 1.24 and 1.07, respectively, corresponding to an order magnitude enhancement in fracture energy.

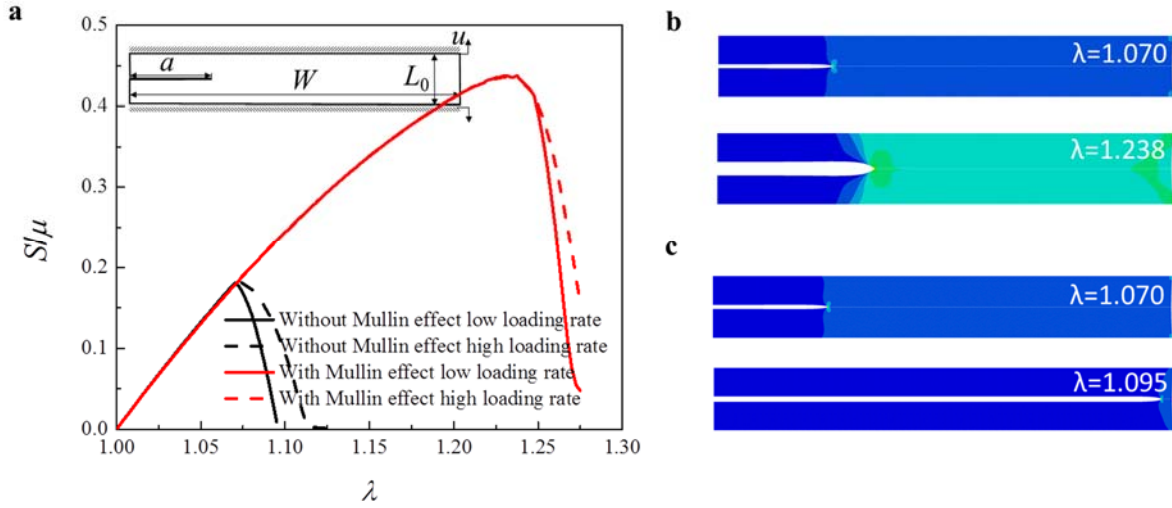


Figure S2. Numerical simulations for the toughening effect of energy dissipation. (a) Stress-stretch curves for materials with and without Mullins effect. The inset figure is the schematic show of the simulated model. (b) Snapshots for the crack initiation and propagation in the materials with Mullins effect ($h_{\max}=0.858$). The crack initiates at the stretch level of 1.07, but does not propagate until the stretch level of 1.24 due to the effect of mechanical energy dissipation. (c) Snapshots for the crack initiation and propagation in the materials without Mullins effect. The crack initiates and propagates at the stretch level of 1.07.

We next validate the choices of the stiffness of the cohesive zone k and mesh size used in the simulations. The simulated sample contains 70,000 elements when using minimum mesh size as 0.1 mm. It is very difficult to further reduce the mesh size with the current available computational resources for us. We thus choose a smaller sample ($L_0=20$ mm, $W_0=160$ mm, and $a=40$ mm) for the validation. As demonstrated in **Fig. S3a**, the stress-stretch curves converge to

a single curve for large enough stiffness of the cohesive zone (i.e., $k/S_{\max} > 15$). Therefore, we set the stiffness of cohesive zone k is always at least 15 times larger than S_{\max} in the simulations to eliminate the influence of the cohesive layer on the mechanical response of the materials. As shown in **Fig. S3b**, simulations with two different mesh sizes (0.1 and 0.05 mm) are in good agreement with each other, indicating that our results are insensitive to the mesh size (0.1 mm) adopted in current simulations.

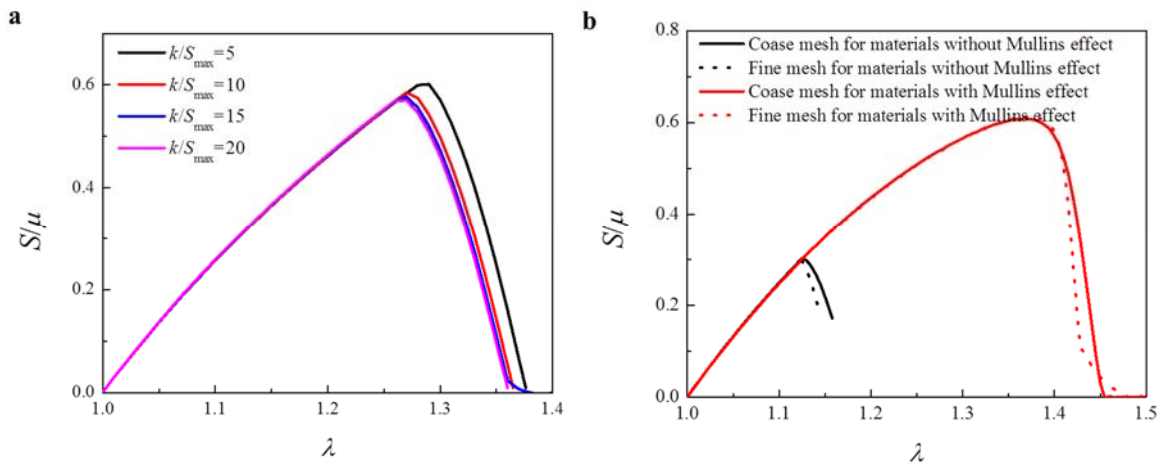


Figure S3. Validation of the finite element models. (a) Effect of the stiffness value of the cohesive zone k on the simulations. (b) Effect of mesh size on the simulations.

Material preparation and mechanical test

To validate the proposed theory and model, we take the interpenetrating-network hydrogel of PAAm-Alginate as a model material to investigate the toughness enhancement due to energy dissipation in a realistic soft material. A pre-gel solution is prepared by mixing 4.1 mL 4.8 wt% alginate (Sigma, A2033) and 5.5 mL 18.7 wt% acrylamide (Sigma, A8887). We add 900 μ L

0.2g/100ml N,N-methylenebisacrylamide (Sigma, 146072) as the crosslinker for polyacrylamide and 102 μL 0.2 M ammonium persulphate (Sigma, 248614) as a photo initiator for polyacrylamide. After degassing the pre-gel solution in a vacuum chamber, we add respectively 200 μL and 300 μL (sample 1: 200 μL ; sample 2: 300 μL) 1 M calcium sulphate (Sigma, C3771) as the crosslinker for alginate and 8.2 μL N,N,N',N'-tetramethylethylenediamine (Sigma, T7024-50M) as the crosslinking accelerator for polyacrylamide to form hydrogels with different energy dissipation. Thereafter, the pre-gel solution is infused into a glass mold and is subjected to ultraviolet light for 60 minutes with 8 W power and 254 nm wavelength to cure the hydrogel. Pure-shear tension test is applied on the samples with Zwick/Roell Z2.5 materials testing machine at room temperature. The hydrogel strip for experimentally measuring the fracture energy has a dimension of $L_0=20$ mm, $W_0=180$ mm and $a =90$ mm, which also applies to the numerical simulations presented in **Fig. 5** and **Fig. S5**. As demonstrated by previous study [3], the current size is large enough to obtain fracture energies that are independent of the specimen size.

Digital image correlation

As illustrated by **Fig. S4**, digital image correlation is a non-contact optical technique that allows full-field strain measurement on a surface under deformation [4]. A random speckle pattern is generated on the surface of a sample by spray painting. Images of speckle patterns at both reference state and deformed state were recorded by a standard video camera during the process of the deformation. Both images are transformed to grey matrices. To track the surface displacements of deforming materials, a mathematically well-defined correlated function is applied to match digitalized images before deformation and after deformation [5]

$$r(x, y) = 1 - \frac{\sum A(x, y)B(x^*, y^*)}{(\sum A(x, y)^2 * \sum B(x^*, y^*)^2)^{1/2}}, \quad (\text{S2})$$

where $A(x, y)$ is the grey level at the location of (x, y) at reference state, $B(x^*, y^*)$ represents the grey level at the location of (x^*, y^*) at deformed state. The relation between (x^*, y^*) and (x, y) can be related as:

$$\begin{cases} x^* = x + u + \frac{\partial u}{\partial x} \Delta x + \frac{\partial u}{\partial y} \Delta y \\ y^* = y + v + \frac{\partial v}{\partial x} \Delta x + \frac{\partial v}{\partial y} \Delta y \end{cases}, \quad (\text{S3})$$

where u and v respectively represents the displacements in the direction of x and y . The displacements can be determined by minimizing the correlated function $r(x, y)$.

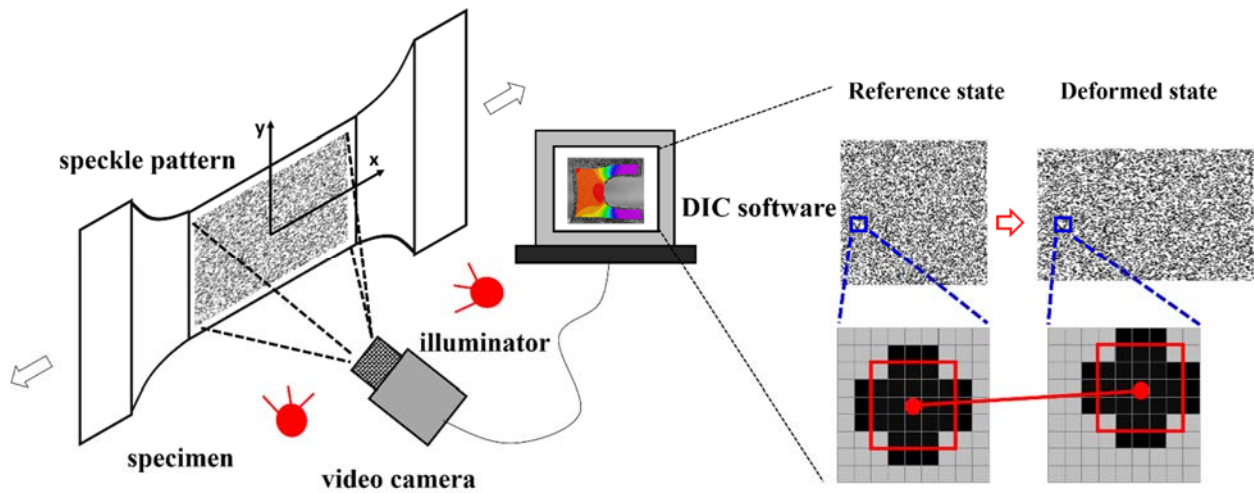


Figure S4. Schematic of digital image correlation technique. A random speckle pattern is spray painted onto the surface of a sample. Images of the speckle patterns at both the reference state and deformed state are recorded by a standard video camera throughout sample extension.

The surface strain is measured by matching the digitalized images before and after deformation via VIC-2D software.

Experimental validation with hydrogel sample 2

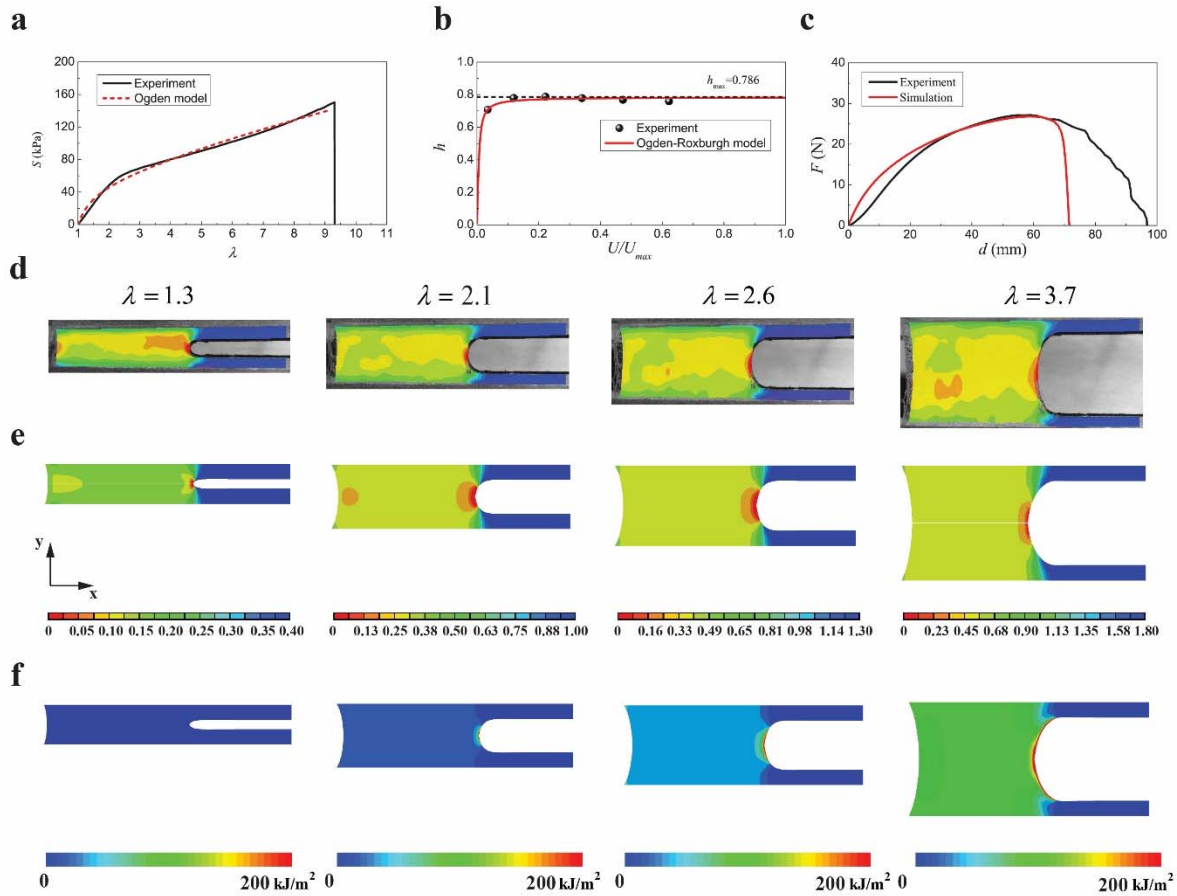


Figure S5. Comparison between experiments and simulations on fracture of PAAm-alginate hydrogel Sample 2. (a) Stress-stretch curves of the sample under pure-shear tensile deformation and one term Ogden model, i.e., $\tilde{W} = 2\mu/\alpha_1^2 (\lambda_1^{\alpha_1} + \lambda_2^{\alpha_1} + \lambda_3^{\alpha_1} - 3)$, with $\mu = 26.49$ kPa and $\alpha_1 = 1.674$. (b) The measured hysteresis ratios of the material deformed to different stretches, and the calculated hysteresis ratio by the modified Ogden-Roxburgh model with $r=1.203$ and $m=4.119$ J/m³. (c) Force-displacement curves of the notched sample under pure-shear test

measured from the experiment and predicted by the model. The strain field in the notched sample under pure-shear test to different stretches: (d) measured by DIC in the experiment and (e) predicted by the model. (f) Energy dissipated in the notched sample under pure-shear test to different stretches. The color represents the true strain (ϵ_{yy}) in (d) and (e) and the density of the energy dissipation in (f).

Supplementary movie. Comparison between experiments and simulations on fracture of PAAm-alginate hydrogel Sample 1. The counter represents the true strain (ϵ_{yy}).

Additional Reference

- [1] R. Rivlin and A. G. Thomas, *Journal of polymer Science* **10**, 291 (1953).
- [2] R. W. Ogden, *Non-linear elastic deformations* (Courier Dover Publications, 1997).
- [3] J.-Y. Sun, X. Zhao, W. R. Illeperuma, O. Chaudhuri, K. H. Oh, D. J. Mooney, J. J. Vlassak, and Z. Suo, *Nature* **489**, 133 (2012).
- [4] W. Peters and W. Ranson, *Optical Engineering* **21**, 213427 (1982).
- [5] H. Bruck, S. McNeill, M. A. Sutton, and W. Peters Iii, *Experimental Mechanics* **29**, 261 (1989).